Temperature dependence of the upper-branch polariton population in an organic semiconductor microcavity

David M. Coles
Department of Physics and Astronomy, University of Sheffield, Hicks Building, Hounsfield Road, Sheffield S3 7RH, United Kingdom

Paolo Michetti
Institute of Theoretical Physics and Astrophysics, University of Wurzburg, D-97074 Wurzburg, Germany

Caspar Clark
Helia Photonics, Rosebank Park, Livingston, West Lothian EH54 7EJ, United Kingdom

Ali M. Adawi* and David G. Lidzey†
Department of Physics and Astronomy, University of Sheffield, Hicks Building, Hounsfield Road, Sheffield S3 7RH, United Kingdom
(Received 5 April 2011; published 18 November 2011)

We explore the distribution of polaritons along the upper polariton branch of a strongly coupled organic-semiconductor microcavity as a function of temperature following nonresonant optical excitation. Measurements of polariton emission from a high-finesse cavity containing a thin film of a J-aggregated cyanine dye were performed as a function of external detection angle and temperature and compared with the results of detailed numerical simulations. We show that a full description of temperature-dependent upper-branch polariton emission can only be obtained by accounting for the interplay between two mechanisms that populate polariton states, namely, thermally assisted exciton scattering and direct radiative pumping of the photonic component of polariton states via the radiative decay of weakly coupled "reservoir" excitons. Our measurements provide a full description of the basic mechanisms at play in an organic microcavity, and may help guide the development of organic polariton-based devices.

DOI: 10.1103/PhysRevB.84.205214 PACS number(s): 78.20.−e, 78.55.Kz, 78.60.Lc, 78.67.Pt

I. INTRODUCTION

When a thin film of a semiconductor material with a narrow absorption linewidth is placed within a high-finesse optical cavity such that the exciton energy of the semiconductor is resonant with the energy of confined photons, strong coupling can occur between excitons and photons forming new quasiparticle states termed cavity polaritons.[1] Strong coupling is evidenced by the observation of an energetic anticrossing between exciton- and cavity-photon modes, with the formation of upper and lower polariton branches (UPB and LPB) that are split in energy around the uncoupled exciton energy.[2] The energetic separation of the polariton branches at exciton-photon resonance is the Rabi splitting energy and is a measure of the coupling strength. The polariton branches can be observed in angular-dependent measurements due to the angular dependence of the energy of the confined cavity-photon mode. The mixed exciton-photon nature of polaritons results in them having an effective mass of approximately 10^{-4} that of an electron,[3] and so collective nonlinear effects are readily achievable. Observed polariton phenomena include the formation of a nonequilibrium Bose-Einstein condensate,[4] parametric amplification,[5] polariton lasing following optical pumping,[6] and polariton emission following electrical pumping.[7] Strong coupling in an optical microcavity (MC) has been observed using a range of different semiconductor materials, including III-V and II-VI semiconductor quantum wells,[1,8–10] bulk semiconductor materials,[11,12] and organic semiconductor thin films.[13–15] Organic semiconductor MCs are now receiving attention as a potential route to create an electrically pumped organic laser. Electrical excitation of organic polaritons has already been demonstrated,[16] and, recently, lasing has been evidenced from a strongly coupled MC containing a thin film of the organic semiconductor anthracene.[17]

A number of recent experimental[18–21] and theoretical[22–26] studies have now addressed the basic physics of strongly coupled organic semiconductor cavities. In many such structures, positional and energetic disorder within the active optical layer results in the strong-coupling regime being limited to long in-plane wavelength Fourier components.[27] The consequence of this is that delocalized polariton states coexist with a large number of uncoupled (or weakly coupled) excitons. The density of states (DOS) of these uncoupled excitons is similar to that of a bare optically active film. It is thought that following nonresonant excitation of an organic microcavity, excitations accumulate at the bottom of the uncoupled exciton DOS, forming exciton "reservoir" (ER) states.[18,22–25,27–30] Following the population of such reservoir states, the formation of polaritons can occur via scattering from the ER, and thus the energetic distribution of states within the ER plays a crucial role in determining polariton populations. We have recently shown that the population of polariton states that are lower in energy than the ER (i.e., states along the lower polariton branch) involves the scattering of an exciton initially in the ER with emission of energy in the form of a vibrational quantum.[21] The scattering mechanisms required to populate polariton states higher in energy than the ER (i.e., in the UPB) are less well understood. Previously, we[31] and others[19,32] have shown that the UPB emission from an organic-semiconductor MC is

temperature activated. These observations provide evidence that the population of the UPB states involves thermally assisted scattering of excitons from the ER states. It has, however, been proposed[24,25,27,29,30,33] that a second mechanism may be important in the population of UPB polaritons, namely, a radiative pumping process originating from the spontaneous emission of photons by weakly coupled excitons in the ER. In this paper, we present evidence that highlights the interplay between such radiative and nonradiative scattering mechanisms and their role in populating states in the UPB. This understanding is facilitated using a detailed theoretical model to describe the generation and relaxation of excitons within the ER and their subsequent scattering into polariton states. This is compared with experimental measurements of the luminescence emission intensity from a negatively detuned MC (i.e., the uncoupled photon energy at normal incidence is less than the exciton energy) as a function of temperature and external measurement angle. We show that the distribution of polariton states along the UPB is approximated by a Maxwell-Boltzmann distribution at room temperature. At low temperatures, however, the UPB population no longer assumes a Maxwell-Boltzmann distribution, as a significant fraction of polaritons close in energy to the exciton reservoir are instead generated following the radiative decay of reservoir excitons that "pump" the photon component of the polaritons. While the nonlinear and collective effects observed in inorganic MCs have principally involved states on the LPB, the effects observed here on the UPB permit us to accurately describe the dynamics of both upper and lower branch states, and thereby quantify the importance of the ER. We note that the improved understanding that we present here will also be of particular importance when studying positively detuned MCs (uncoupled photon energy at normal incidence is greater than the exciton energy), as the bottom of the LPB directly overlaps with the ER and thus the optical pumping mechanisms that we highlight are likely to be particularly important. Our results also have relevance for the development of electrically pumped polariton-based devices,[16] in which the states in the ER are directly populated by charge injection.

II. METHODS

A. Experimental methods

The cavity structure we have explored is shown in Fig. 1(a). A distributed Bragg reflector (DBR) consisting of 11 pairs of Nb_2O_5–SiO_2 was grown by ion-assisted physical vapor deposition (PVD) on a fused quartz substrate. A layer of the *J*-aggregate dye 5,6-dichloro-2-[[5,6-dichloro-1-ethyl-3-(4-sulphobutyl)-benzimidazol-2-ylidene]-propenyl]-1-ethyl-3-(4-sulphobutyl)-benzimidazolium hydroxide, sodium salt, inner salt (TDBC) dispersed in a poly(vinyl alcohol) (PVA) matrix was spin cast directly onto the DBR to a thickness of 220 nm. A second DBR symmetric to the first was then grown directly on top of the organic layer to complete the cavity. We have used TDBC as the active organic semiconductor in our microcavities, as under suitable preparation conditions it is able to form *J* aggregates with absorption and emission that are spectrally red-shifted and greatly narrowed compared to the monomer. The absorption and photoluminescence (PL) of

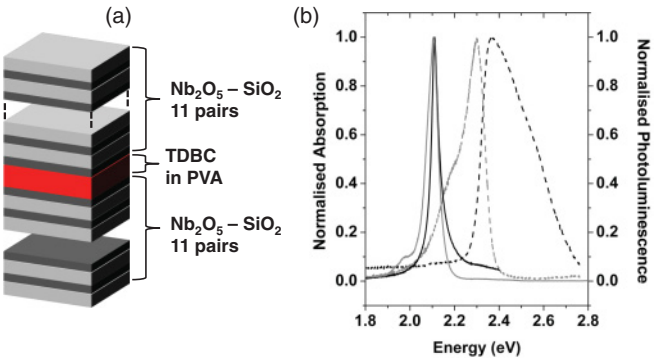

FIG. 1. (Color online) (a) Microcavity structure consisting of TDBC *J* aggregates in a PVA matrix between two niobia-silica DBRs consisting of 11 $\lambda 7/4$ pairs. (b) Normalized absorption (black lines) and photoluminescence (gray lines) of TDBC *J* aggregates in a PVA matrix (solid lines) and monomer in methanol (dashed lines).

TDBC in both its monomeric and aggregated form is shown in Fig. 1(b). The monomer was prepared by dissolving the dye in methanol, with absorption (photoluminescence) peaking at 2.38 (2.30) eV and having a linewidth of 272 (136) meV. When TDBC is dissolved in an aqueous solution, *J* aggregates are formed[34,35] with absorption (photoluminescence) peaking at 2.11 (2.10) eV and having a linewidth of 50 (50) meV. Adding the polymer poly(vinyl alcohol) to the aqueous solution allows thin films of *J* aggregates supported within an optically transparent polymer matrix to be spin cast. The strong narrowing of emission, which is also accompanied by an increase in relative oscillator strength, is a desirable attribute for optical strong-coupling applications, as is the small Stokes shift.[36] The microcavities fabricated were characterized using angular- and temperature-dependent PL measurements. For measurement, the cavity was mounted in a liquid-nitrogen-cooled cryostat with temperature control and wide-angle optical access, centered on the rotation axis of a goniometer. Light collection optics were mounted on a rotating arm. The rotation of the PL collection arm was controlled by a programmable stepper motor, allowing high resolution and repeatable control over collection angle. Nonresonant excitation for photoluminescence was provided by means of a 40-mW HeCd laser (2.81 eV) focused on the sample surface at normal incidence to a spot size of 100 μm. Emission spectra were collected every 0.2° between the angles of 10° and 55° over a solid angle of 3.8 msr. The sample temperature was varied between 77 and 293 K.

B. Theoretical methods

To understand the PL emission from our structures recorded following nonresonant excitation, we have used a numerical model that describes the relaxation dynamics in a strongly coupled MC that contains a thin film of a *J*-aggregated organic dye. The model has been described in detail in Refs. 24 and 25, and we refer the reader to the original work for full mathematical details. Briefly, however, we outline its main features. We use a well-established physical picture[37–39] that describes the electronic states of *J* aggregates (a linear aggregate of N_d dye monomers) in terms of a one-dimensional (1D) Frenkel exciton system with on-site energetic disorder.

Without disorder, Frenkel excitons extend along the whole aggregate and are characterized by a J-band dispersion, with the accumulation of the whole aggregate oscillator strength in the lowest-energy superradiant excitons. The superradiant excitons are responsible for the narrow and intense optical absorption of J aggregates that are red-shifted with respect to that of the dye monomer.

In order to calculate the film PL, the model accounts for scattering among exciton states due to the absorption or emission of a vibrational quantum from a thermal bath.[38,39] The relaxation dynamics in a J aggregate are described by a set of coupled rate equations including scattering rates and spontaneous emission rates of excitons, while the population redistribution between different aggregates is assumed unlikely as individual aggregates are suspended in an inert and transparent host matrix and, thus, this process is not included. Because of this, the steady-state exciton population on each individual J aggregate can be approximatively described using a Boltzmann factor, however, the ensemble average over disorder configurations leads to an ER population corresponding to an inhomogeneously broadened sum of Boltzmann distributions. The PL following nonresonant pumping can be obtained by solving the ensemble average of the steady-state population.

In the strong-coupling regime, superradiant excitons mix with cavity-photon modes to form exciton polaritons. Figure 2(a) shows a typical polariton dispersion curve calculated using our model. Here, the parameters used have been adjusted to provide good agreement with the experimentally determined polariton dispersion as demonstrated in the following section. Note that we have also added an *ad hoc* rigid shift to the bare exciton resonance in order to reproduce the temperature-induced shift that is observed in the experimental data. In Fig. 2(b), we plot the exciton reservoir density of states (DOS) within the cavity that we calculate using an ensemble average over 5000 disorder configurations. We find this approach to give a reasonable description of the DOS (as determined from the optical absorption of the bare J-aggregate film). We then use our model of the DOS to predict the distribution of states within the ER as shown in Fig. 2(c). Our model indicates that the formation of a quasithermalized population distribution occurs at the bottom of the exciton DOS on a time scale of less than a picosecond. It is from these states that population of states along both polariton branches proceeds on slower time scales (of the order of hundreds of ps). This situation corresponds to a relaxation bottleneck, a feature that shares some similarities with observations made in early experiments on quantum-well MCs.[40,41]

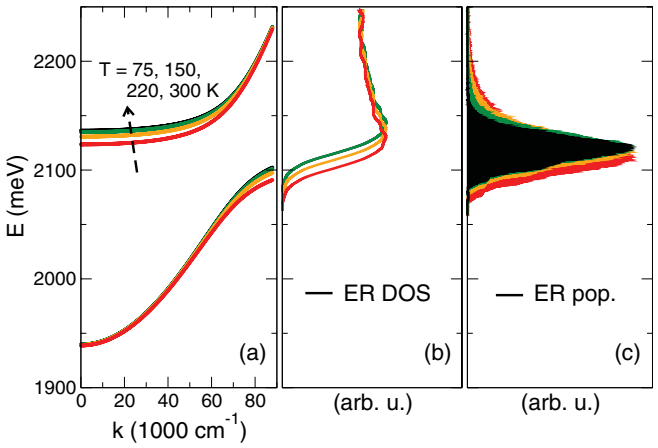

FIG. 2. (Color online) (a) Polariton dispersion curves accounted for in the simulations. (b) J-aggregate film exciton DOS obtained as an ensemble average over 5000 disorder configurations of individual aggregates. (c) ER steady-state population for a J-aggregate film inside a MC as determined by the simulations. All data are shown for $T = 75$, 150, 220, and 300 K.

Our model accounts for the scattering by including emission or absorption of energy and momentum mediated by a thermal bath of vibrations, active between all the excited states of the system (polaritons and uncoupled excitons). This bath of thermal vibrations (the energy of which is limited to a maximum value of 10 meV) is assumed to be composed of a continuous spectrum of low-energy molecular vibrations.[38,39] We make no *a priori* assumptions of their origin, although these may be associated with the J aggregate or with the host matrix. In addition, we also include a series of higher-energy vibrational modes that correspond to the dominant Raman-active modes of the TDBC cyanine dye.[42] The modes included have an energy of $E_v = 40$, 80, 120, 150, 185, and 197 meV. We have found that these discrete energy vibrations play a crucial role in the relaxation of reservoir excitons and thus help determine the polariton population distribution along the LPB.[21]

The presence of disorder in the J-aggregate layer introduces a new scattering mechanism as the entire oscillator strength is no longer concentrated in the superradiant exciton states found at the bottom of the ER, but is instead distributed over a wider spectral range of the J-aggregate DOS.[43] Disorder is also known to break the in-plane wave-vector conservation in the coupling between photons and excitons.[27] This induces the formation of a broad distribution of excitonlike states that are partially localized between the UPB and the LPB and have a small but finite coupling with the photon modes.[23] Such states (due to finite exciton and photon lifetime) operate in the weak light-matter coupling regime and have an energy similar to that of the bare exciton and therefore exist within the ER. Such weakly coupled states are, however, able to optically pump the photon component of the polaritons following radiative decay and thus provide a further mechanism to generate a polariton population. It is difficult to provide a quantitative measure of the fraction of ER states that carry only residual oscillator strength due to the complexity of the system. To account for this, however, we simulate the optical pumping of polaritons via radiative decay of weakly coupled excitons from the bare-film photoluminescence multiplied by both the photon fraction of the final polariton state[24,25] and by the fitting parameter β.[44] In our simulations, we have found that a value of $\beta = 0.4$ times that of the emission intensity of the control film was needed to accurately reproduce the experimental data.

III. EXPERIMENTAL RESULTS

In Figs. 3(a) and 3(b), we plot the angular-dependent PL emitted by the cavity at 77 and 293 K. For each angular measurement, we fit the spectrum with three Lorentzian

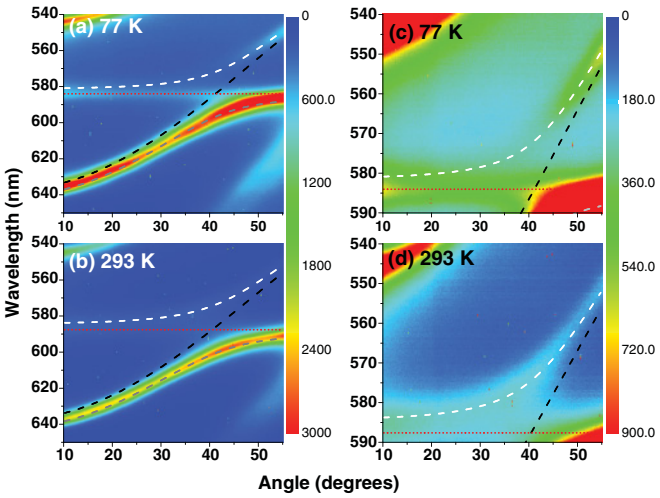

FIG. 3. (Color online) Cavity PL as a function of angle at (a) 77 K and (b) 293 K. UPB emission at (c) 77 K and (d) 293 K [rescaled from (a) and (b)]. Two-level model fit of the UPB, LPB, photon and exciton energies are shown with dashed white, gray, black, and dotted red lines, respectively.

lineshapes representing the emission of states in the UPB, LPB, and ER. We fit the angular-dependent energy of the UPB and LPB emission energy to a two-level model [Eq. (1)], which treats the cavity photon and excitons as classically coupled oscillators.[45] This model also allows the photonic (excitonic) fraction of the UPB (LPB) polaritons (α^2) to be calculated via Eq. (2):

$$E_{\mathrm{pol}}(\theta) = \frac{E_\gamma(\theta) + E_X}{2} \pm \frac{1}{2}\sqrt{(E_\gamma(\theta) - E_X)^2 + (\hbar\Omega_{\mathrm{Rabi}})^2} \tag{1}$$

$$\alpha^2(\theta) = \frac{E_\gamma(\theta) - E_{\mathrm{pol}}(\theta)}{E_X + E_\gamma(\theta) - 2E_{\mathrm{pol}}(\theta)}, \tag{2}$$

where E_{pol} is the polariton energy, E_X is the exciton energy, $\hbar\Omega_{\mathrm{Rabi}}$ is the Rabi splitting energy, and E_γ is the cavity-photon energy given by $E_\gamma(\theta) = E_0(1 - \frac{\sin^2\theta}{n^2})^{-\frac{1}{2}}$, where E_0 is the cavity-mode energy at normal incidence, θ is the observation angle relative to the sample normal, and n is the effective intracavity refractive index. We find that the cavity has a Rabi splitting energy of 97 meV and detuning (defined as the energy difference between the uncoupled exciton and photon energies at 0°) of −164 meV.

It can be seen that the emission from the cavity is dominated by PL emitted from the LPB, with emission from the UPB being around 20 times weaker than that from the LPB. We have previously characterized the emission from the lower polariton branch in detail[21] and, thus, we do not discuss this in detail here. Briefly, however, it was shown that thermalized reservoir excitons can scatter to states along the lower polariton branch by losing excess energy to the various vibrational modes of the TDBC dye. Despite this scattering mechanism, a bottleneck exists following nonresonant excitation whereby the majority of polariton states populated are close in energy to the exciton reservoir.

In Figs. 3(c) and 3(d), we replot and rescale the emission emitted from the UPB following nonresonant excitation at 77 and 293 K. It is clear that, at 293 K, luminescence is observed from the UPB at all angles with a progressive weakening observed at increasing angles. At 77 K, the cavity emission pattern changes markedly, with emission from the UPB being confined to external viewing angles below 20° and above 45°. We first address the strong increase in emission seen at low temperatures at angles above 45°. In Fig. 4(a), we plot the PL emission of a control thin film of TDBC J aggregates as a function of temperature. Two main effects are visible. First, the intensity of PL emission from the J band increases by almost 3.5 times as the temperature is reduced from 293 to 77 K. A similar observation has also been reported in thin films of J aggregates of a carbocyanine dye, and has been assigned to a thermal competition between emission from radiative self-trapped excitons and nonradiative excitons having large values of center-of-mass wave vector.[46] Most importantly, however, we also observe a growth in emission intensity of a broad band that peaks at approximately 200 meV above that of the main J band. By comparison with the PL emission spectrum presented in Fig. 1(b), this feature appears to correspond to TDBC monomer emission. We can associate the observed increase in monomer emission with the increased emission from the microcavity at large angles and low temperatures by plotting the peak intensity of the monomer emission band as a function of temperature in Fig. 4(b) together with the relative intensity of luminescence emitted from the cavity at 550 nm (2.26 eV). It can be seen that both emission features have a similar temperature dependence, suggesting that emission from the UPB at low temperatures and at viewing angles of $\theta > 45°$ corresponds to weakly coupled monomer emission from TDBC that "leaks" through the photonlike polariton mode. It should be noted that there is negligible change in the UPB photon fraction at 550 nm over the temperature range studied, confirming that the observed emission is due to a change in photoluminescence intensity from within the cavity rather than a change in photonic fraction of the UPB.

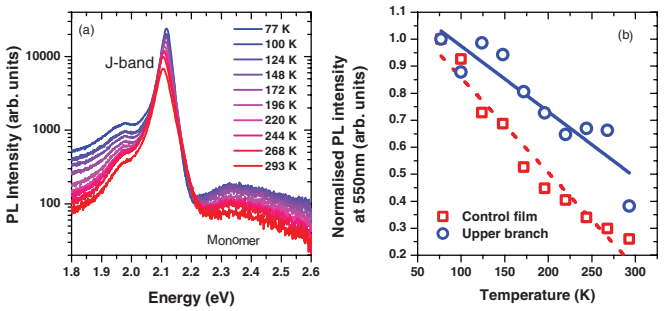

FIG. 4. (Color online) (a) Temperature-dependent TDBC emission. (b) Control film emission intensity (red squares) and upper branch emission intensity (blue circles), both at 550 nm.

We now turn our attention to the polariton emission from the UPB at viewing angles $\theta < 45°$ in which the emission from uncoupled cyanine dye monomers does not "pollute" the polariton emission signal. The emission intensity from the UPB [$I_{\mathrm{UPB}}(\theta, T)$] can be converted to a value proportional to the polariton population (N_{UPB}) by dividing by the photonic fraction of the polariton state as calculated from Eq. (2). In Fig. 5, the polariton population is plotted as a function of the difference between the the UPB energy [$E_{\mathrm{UPB}}(\theta, T)$] and

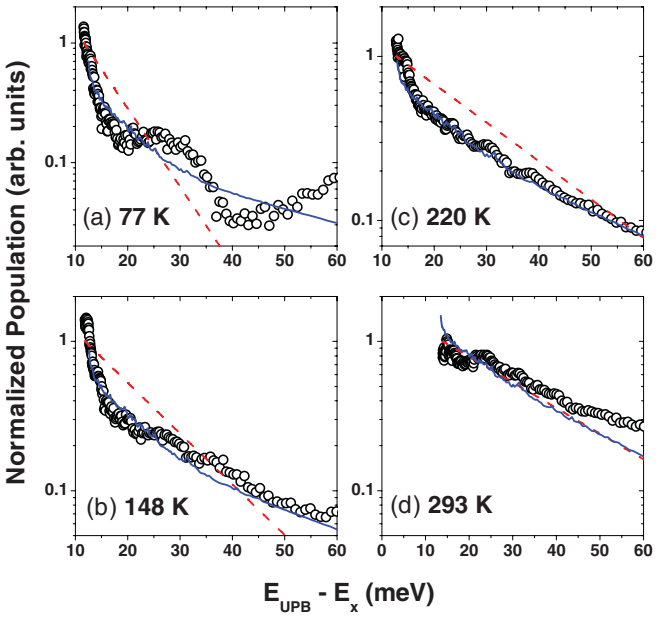

FIG. 5. (Color online) UPB population (empty circles) as a function of energy splitting from the exciton reservoir for a series of temperatures. Red dashed lines are a Maxwell-Boltzmann distribution and blue solid lines are the result of our model.

exciton energy $[E_X(T)]$ for a series of temperatures (open circles). Here, we assume the exciton-reservoir energy is within 12 meV of the energy of the peak of the J-aggregate optical absorption.[43] The polariton population is normalized to its maximum value observed close to the exciton energy [i.e., where $E_{\mathrm{UPB}}(\theta,T) - E_X(T)$ is small]. It can be seen that, in all cases, the polariton population undergoes a progressive reduction as the energy separation between the UPB and the exciton reservoir increases. We can explore the form of this population distribution by plotting a Maxwell-Boltzmann distribution $[N_{\mathrm{UPB}} = \exp(-\frac{E_{\mathrm{UPB}}-E_X}{k_B T})]$ as shown using a red line. It can be seen that, at high temperature (293 K), we obtain a reasonable description of the observed population distribution. As the temperature is reduced, however, the deviation from a simple Maxwell-Boltzmann distribution increases. In order to understand the origin of the polariton population distribution and its temperature dependence, it is clear that we need to go beyond a simple statistical distribution. In the next section, we show that the numerical model described above provides an improved description of the temperature-dependent polariton emission, and confirms the presence of two competing mechanisms that populate states along the UPB.

IV. NUMERICAL SIMULATIONS

We have used our model to predict the scattering mechanisms both to and from the UPB and the ER as a function of energetic separation between each polariton state and the bottom of the exciton reservoir ($E_{\mathrm{UPB}} - E_X$) and as a function of temperature. This has been done for both the radiative and nonradiative scattering mechanisms described above, as shown in Fig. 6. Here, we assume a relatively low continuous pumping rate of 6.5×10^7 s^{-1} of each aggregate on the high-energy wing of the exciton J band, with the aggregates

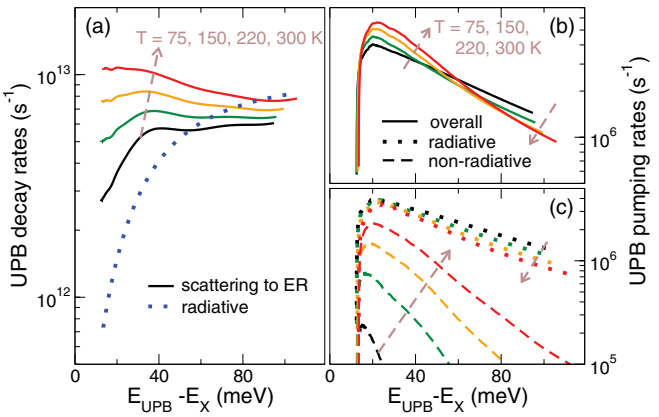

FIG. 6. (Color online) (a) Decay rates of exciton polaritons due to PL emission (dotted line) and to scattering back into the ER with emission or absorption of a vibration for different temperatures (full lines). (b) Overall *average* scattering rate to the UPB for an excitation in the ER. (c) The individual contribution of the radiative (dotted lines) and nonradiative (dashed lines) mechanism to the overall *average* scattering rate from the ER to the UPB. Dashed arrows indicate the trend of the data on increasing temperature from $T = 75$ to 300 K.

being spatially separated by an average distance of $R = 200$ Å. Figure 6(a) shows the decay rate of the UPB by scattering back to the ER through the emission of energy in the form of a vibrational quanta (solid lines). This temperature-dependent process happens over time scales of the order of 150 fs and has been determined experimentally at room temperature.[20,27] The plot also shows the relative UPB decay rate through radiative decay to the outside world (dotted line). This decay rate of UPB states is dependent on the relative photon fraction of each polariton state. In our model, we assume an "uncoupled" photon lifetime in our cavity of 100 fs, a value consistent with the measured Q factor of our cavities of approximately 300. Note that polariton PL is the only sink of excitations included in our model. We do not discount the presence of other decay processes (e.g., exciton-exciton annihilation or radiative decay of reservoir excitons through leaky modes of the cavity), however, these processes simply reduce the steady-state population density in the cavity but leave the relative occupation of the ER, UPB, and LPB unchanged. Figure 6(b) shows the overall scattering rate from the ER to the UPB, averaged over the steady-state ER population. $\Gamma(E)$ measures the average rate at which a particle in the ER scatters into a UPB state of energy E:

$$\Gamma(E) = \frac{\left\langle \sum_i n_i W_{i\to \mathrm{UPB}}(E) \right\rangle}{\left\langle \sum_i n_i \right\rangle}, \tag{3}$$

where i runs over all J-aggregate exciton states, n_i is the steady-state population, $W_{i\to\mathrm{UPB}}$ the scattering rate from the ith exciton to the UPB, and is ensemble averaged over the disorder configurations. In Fig. 6(c), we plot the various contributions to this scattering process from both the radiative mechanism (dotted lines) and nonradiative scattering (dashed lines). In all cases, rates are shown as a function of temperature. It can be seen that the nonradiative scattering mechanisms that rely on the absorption of a vibrational quantum are extremely sensitive to temperature [see Fig. 6(c)], as they

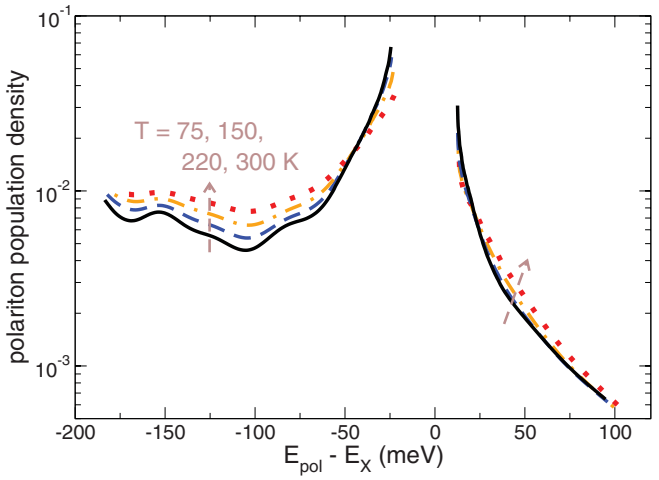

FIG. 7. (Color online) Polariton population density obtained solving the steady-state condition for the numerical model for a range of different temperatures. Details are given in the text.

are dependent on the population of the thermal bath of vibrations and therefore are subject to thermal activation. The radiative scattering processes are only weakly temperature dependent, with their relative efficiency reflecting the relative balance between weakly coupled and superradiant states in the reservoir. It can be seen that the radiative mechanism is weakly deactivated with temperature because increasing T leads to the thermal population of high-energy states in the ER that carry a negligible oscillator strength and that, therefore, do not contribute to the radiative pumping of polaritons.

In Fig. 7, we plot the steady-state polariton population density along the LPB and the UPB obtained by our simulations. It can be seen that the population density along the LPB (which is on average 10^{-2}) contains a number of pronounced resonances that occur at energies $E_X - E_{\mathrm{LPB}} \approx E_v$, where E_v is the energy of one of the vibrational modes of the J aggregates. Such features have recently been observed experimentally in angular-dependent measurements of PL emission intensity along the LPB of a J aggregate containing microcavity.[21] Our simulations indicate that at $T = 75$ K, the number of excitations per aggregate is $N_{\mathrm{agg}} = 3.8 \times 10^{-2}$ and the fraction of the population distributed over polariton states is $\chi = 6.0 \times 10^{-4}$ (i.e., the majority of the population is located in the ER). At room temperature, the population is more spread over the UPB and LPB, being enhanced away from E_X compared to its low-temperature value and suppressed near E_X, with $N_{\mathrm{agg}} = 5.0 \times 10^{-2}$ while $\chi = 3.4 \times 10^{-4}$.

V. DISCUSSION

We now compare the results of our simulations with experimentally determined polariton population determined along the UPB as shown in Fig. 5. Here, the steady-state polariton population for each temperature calculated using the model is shown using a solid blue line. It can be seen that, at all temperatures, the population of polaritons below resonance (occurring around $E_{\mathrm{UPB}} - E_X = 60$ meV) are reasonably well described by our model. In particular, the model correctly describes the sharp increase in population that occurs for energetic separations of < 20 meV between the UPB and the exciton reservoir. It can be seen that the population distribution at this point is not well described by a simple MB distribution, suggesting that, at low temperature, the relative population of such states is strongly determined by the radiative pumping mechanism. We have argued that the UPB population is dependent on two competing mechanisms: first, a thermal promotion of excitons from the reservoir into polariton states that occurs via interactions with a "thermal bath" of low-energy vibrational modes [Fig. 6(c) dashed lines]. Such a thermal bath will have a population given by a Bose-Einstein distribution and will, hence, be strongly affected by temperature (being enhanced at high temperatures). The second mechanism is the optical pumping of polariton states via radiative decay of weakly coupled reservoir excitons [Fig. 6(c) dotted lines]. This mechanism is assumed to be proportional to the relative emission intensity of the control film as shown in Fig. 4.[24,25,29,30,33] The radiative pumping mechanism is thus expected to dominate at low temperatures, although only for polariton states having an energy that overlaps with the exciton emission. As can be seen in Fig. 6(c), radiative scattering is the dominant scattering mechanism that occurs at low temperature. However, nonradiative scattering is strongly temperature activated and, at room temperature, is of the same order of magnitude as radiative scattering. Indeed, at sufficiently high temperature, the ultrafast decay of UPB polaritons back to the ER becomes significantly faster than polariton radiative decay [see Fig. 6(a)]. This fast UPB decay process has two main consequences. First, it explains the relative weakness of UPB emission, an observation consistent with the broader linewidth of the UPB compared to the LPB. Second, it results in improved thermalization of the ER and the UPB at high temperature, with the UPB population approximating a Maxwell-Boltzmann distribution as seen in Fig. 5(d). We note that the radiative scattering process studied here is anticipated to be of crucial importance in positively detuned MCs, where they can be used to directly generate a polariton population at the bottom of the LPB where collective phenomena are expected to occur. Indeed, recent experiments[47] have demonstrated the existence of a thermalized polariton population at the bottom of the LPB by including a thin film of a resonant weakly coupled fluorescent dye in the cavity, which is able to optically pump the LPB.

VI. SUMMARY AND CONCLUSIONS

We have studied the photoluminescence emission from a strongly coupled microcavity containing a thin film of a J-aggregated cyanine dye as a function of external viewing angle and temperature. We have concentrated our studies on emission from the upper polariton branch, and have shown that the population of polariton states is dependent on both a thermally assisted exciton scattering mechanism and an optical pumping mechanism due to the radiative decay of weakly coupled reservoir excitons. The relative importance of such processes is determined by temperature, with radiative pumping being enhanced at low temperature and thermally assisted population becoming increasingly important at high

temperatures. Our work confirms the importance of the reservoir of uncoupled exciton states in determining the steady-state distribution of polaritons, and confirms the importance of a radiative pumping mechanism to generate polariton states, the energies of which overlap with states in the exciton reservoir. This understanding will be of crucial importance in devising efficient electrically driven polariton devices or understanding the optical properties of positively detuned microcavities.

ACKNOWLEDGMENTS

We gratefully acknowledge funding of this work via the UK EPSRC via Grant No. EP/G062404/1, and via the 7th Framework ITN project Icarus (237900). D.C. thanks the UK ESPRC for the award of a DTA scholarship. P.M. thanks the DFG for financial support via Emmy Noether program (Grant No. RE 2978/1-1). We also thank P. Lagoudakis and P. Savvidis for helpful discussions.

*Current address: Department of Physics, University of Hull, Cottingham Road, Kingston-upon-Hull HU6 7RX, United Kingdom.

†d.g.lidzey@sheffield.ac.uk

[1] C. Weisbuch, M. Nishioka, A. Ishikawa, and Y. Arakawa, Phys. Rev. Lett. **69**, 3314 (1992).

[2] Y. Yamamoto, F. Tassone, and H. Cao, *Semiconductor Cavity Quantum Electrodynamics* (Springer, Berlin, 2000).

[3] M. Richard, J. Kasprzak, R. André, R. Romestain, L. S. Dang, G. Malpuech, and A. Kavokin, Phys. Rev. B **72**, 201301 (2005).

[4] J. Kasprzak, M. Richard, S. Kundermann, A. Baas, P. Jeambrun, J. M. J. Keeling, F. M. Marchetti, M. H. Szymanska, R. Andre, J. L. Staehli, V. Savona, P. B. Littlewood, B. Deveaud, and L. S. Dang, Nature (London) **443**, 409 (2006).

[5] P. G. Savvidis, J. J. Baumberg, R. M. Stevenson, M. S. Skolnick, D. M. Whittaker, and J. S. Roberts, Phys. Rev. Lett. **84**, 1547 (2000).

[6] L. S. Dang, D. Heger, R. André, F. Bœuf, and R. Romestain, Phys. Rev. Lett. **81**, 3920 (1998).

[7] S. I. Tsintzos, N. T. Pelekanos, G. Konstantinidis, Z. Hatzopoulos, and P. G. Savvidis, Nature (London) **453**, 372 (2008).

[8] T. B. Norris, J.-K. Rhee, C.-Y. Sung, Y. Arakawa, M. Nishioka, and C. Weisbuch, Phys. Rev. B **50**, 14663 (1994).

[9] R. Houdré, R. P. Stanley, U. Oesterle, M. Ilegems, and C. Weisbuch, Phys. Rev. B **49**, 16761 (1994).

[10] P. Kelkar, V. Kozlov, H. Jeon, A. V. Nurmikko, C.-C. Chu, D. C. Grillo, J. Han, C. G. Hua, and R. L. Gunshor, Phys. Rev. B **52**, R5491 (1995).

[11] Y. Chen, A. Tredicucci, and F. Bassani, Phys. Rev. B **52**, 1800 (1995).

[12] N. Antoine-Vincent, F. Natali, D. Byrne, A. Vasson, P. Disseix, J. Leymarie, M. Leroux, F. Semond, and J. Massies, Phys. Rev. B **68**, 153313 (2003).

[13] D. G. Lidzey, D. D. C. Bradley, M. S. Skolnick, T. Virgili, S. Walker, and D. M. Whittaker, Nature (London) **395**, 53 (1998).

[14] N. Takada, T. Kamata, and D. D. C. Bradley, Appl. Phys. Lett. **82**, 1812 (2003).

[15] S. Kéna-Cohen, M. Davanço, and S. R. Forrest, Phys. Rev. Lett. **101**, 116401 (2008).

[16] J. R. Tischler, M. S. Bradley, V. Bulović, J. H. Song, and A. Nurmikko, Phys. Rev. Lett. **95**, 036401 (2005).

[17] S. Kena-Cohen and S. Forrest, Nat. Photonics **4**, 371 (2010).

[18] J. Chovan, I. E. Perakis, S. Ceccarelli, and D. G. Lidzey, Phys. Rev. B **78**, 045320 (2008).

[19] G. H. Lodden and R. J. Holmes, Phys. Rev. B **83**, 075301 (2011).

[20] T. Virgili, D. Coles, A. M. Adawi, C. Clark, P. Michetti, S. K. Rajendran, D. Brida, D. Polli, G. Cerullo, and D. G. Lidzey, Phys. Rev. B **83**, 245309 (2011).

[21] D. M. Coles, P. Michetti, C. Clark, W. C. Tsoi, A. M. Adawi, J.-S. Kim, and D. G. Lidzey, Adv. Funct. Mater. **21**, 3691 (2011).

[22] P. Michetti and G. L. Rocca, Phys. E (Amsterdam) **40**, 1926 (2008).

[23] P. Michetti and G. C. La Rocca, Phys. Rev. B **71**, 115320 (2005).

[24] P. Michetti and G. C. La Rocca, Phys. Rev. B **79**, 035325 (2009).

[25] P. Michetti and G. C. La Rocca, Phys. Rev. B **77**, 195301 (2008).

[26] P. Michetti and G. C. La Rocca, Phys. Rev. B **82**, 115327 (2010).

[27] V. M. Agranovich, M. Litinskaia, and D. G. Lidzey, Phys. Rev. B **67**, 085311 (2003).

[28] V. Agranovich, M. Litinskaia, and D. Lidzey, Phys. Status Solidi B **234**, 130 (2002).

[29] M. Litinskaya, P. Reineker, and V. Agranovich, J. Lumin. **110**, 364 (2004).

[30] M. Litinskaya, P. Reineker, and V. Agranovich, J. Lumin. **119-120**, 277 (2006).

[31] S. Ceccarelli, J. Wenus, M. S. Skolnick, and D. G. Lidzey, Superlattices Microstruct. **41**, 289 (2007).

[32] P. Schouwink, J. M. Lupton, H. von Berlepsch, L. Dähne, and R. F. Mahrt, Phys. Rev. B **66**, 081203 (2002).

[33] D. G. Lidzey, A. M. Fox, M. D. Rahn, M. S. Skolnick, V. M. Agranovich, and S. Walker, Phys. Rev. B **65**, 195312 (2002).

[34] E. E. Jelley, Nature (London) **138**, 1009 (1936).

[35] G. Scheibe, Angew. Chem. **49**, 563 (1936).

[36] J. Wenus, L. G. Connolly, and D. G. Lidzey, Phys. Status Solidi C **2**, 3899 (2005).

[37] A. V. Malyshev and V. A. Malyshev, Phys. Rev. B **63**, 195111 (2001).

[38] M. Bednarz, V. A. Malyshev, and J. Knoester, J. Chem. Phys. **117**, 6200 (2002).

[39] M. Bednarz, V. A. Malyshev, and J. Knoester, Phys. Rev. Lett. **91**, 217401 (2003).

[40] R. P. Stanley, R. Houdré, C. Weisbuch, U. Oesterle, and M. Ilegems, Phys. Rev. B **53**, 10995 (1996).

[41] F. Tassone, C. Piermarocchi, V. Savona, A. Quattropani, and P. Schwendimann, Phys. Rev. B **56**, 7554 (1997).

[42] D. M. Coles, A. J. H. M. Meijer, W. C. Tsoi, M. D. B. Charlton, J.-S. Kim, and D. G. Lidzey, J. Phys. Chem. B **114**, 11920 (2010).

[43] A. Armitage, D. G. Lidzey, D. D. C. Bradley, T. Virgili, M. S. Skolnick, and S. Walker, Synth. Met. **111-112**, 377 (2000).

[44] We use for the radiative scattering parameter $\beta = 0.4$. For the continuum of low-energy vibrations, the scattering rate is $\propto \alpha \frac{J}{\hbar}(\frac{E_v}{J})^p$ with $J = 75$ meV the dipole-dipole interaction between dye monomer and the parameter $\alpha = 3.2$ and $p = 0.9$. For the discrete energy vibrations, the vibration energies E_v and coupling

energies γ_v are chosen in $E_v = 40$ ($\gamma_v = 14$), 80 (18), 120 (25), 150 (43), 185 (42), and 197 (67) meV. Note that the comparison with experiments permits us to fix only the relative intensity of the scattering strength, while a reasonable scaling of the strength of all scattering channels of the same factor would leave the results almost unchanged.

[45] M. S. Skolnick, T. A. Fisher, and D. M. Whittaker, Semicond. Sci. Technol. **13**, 645 (1998).

[46] V. F. Kamalov, I. A. Struganova, and K. Yoshihara, J. Phys. Chem. **100**, 8640 (1996).

[47] M. S. Bradley and V. Bulović, Phys. Rev. B **82**, 033305 (2010).